Scopus

Source details

AIP Conference Proceedings

Scopus coverage years: from 1973 to 1978, from 1983 to 1984, 1993, from 2000 to 2001, from 2003 to Present

ISSN: 0094-243X E-ISSN: 1551-7616

Subject area: Physics and Astronomy: General Physics and Astronomy

Source type: Conference Proceeding

View all documents > Set document alert Save to source list

CiteScore 2022
0.7

SJR 2022
0.164

SNIP 2022
0.247

CiteScore CiteScore rank & trend Scopus content coverage

i Improved CiteScore methodology

CiteScore 2022 counts the citations received in 2019-2022 to articles, reviews, conference papers, book chapters and data papers published in 2019-2022, and divides this by the number of publications published in 2019-2022. Learn more >

CiteScore 2022

0.7 = 31,947 Citations 2019 - 2022 / 43,416 Documents 2019 - 2022

Calculated on 05 May, 2023

CiteScoreTracker 2023

0.5 = 19,544 Citations to date / 41,650 Documents to date

Last updated on 05 August, 2023 • Updated monthly

CiteScore rank 2022

Category	Rank	Percentile
Physics and Astronomy — General Physics and Astronomy	#203/240	15th

View CiteScore methodology > CiteScore FAQ > Add CiteScore to your site

AIP Conference Proceedings

COUNTRY

United States

Universities and research institutions in United States

Media Ranking in United States

SUBJECT AREA AND CATEGORY

Physics and Astronomy
└ Physics and Astronomy (miscellaneous)

PUBLISHER

American Institute of Physics

H-INDEX

80

PUBLICATION TYPE

Conferences and Proceedings

ISSN

0094243X, 15517616

COVERAGE

1973-1978, 1983-1984, 1993, 2000-2001, 2003-2022

INFORMATION

Homepage

How to publish in this journal

confproc@aip.org

SCOPE

Today, AIP Conference Proceedings contain over 100,000 articles published in 1700+ proceedings and is growing by 100 volumes every year. This substantial body of scientific literature is testament to our 40-year history as a world-class publishing partner, recognized internationally and trusted by conference organizers worldwide. Whether you are planning a small specialist workshop or organizing the largest international conference, contact us, or read these testimonials, to find out why so many organizers publish with AIP Conference Proceedings.

Join the conversation about this journal

SJR

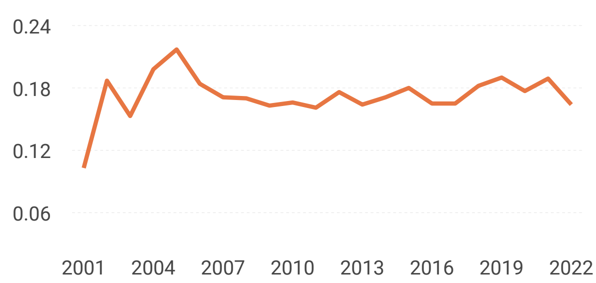

Total Documents

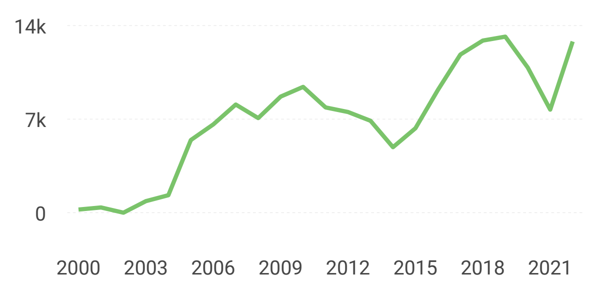

Total Cites Self-Cites

Citations per document

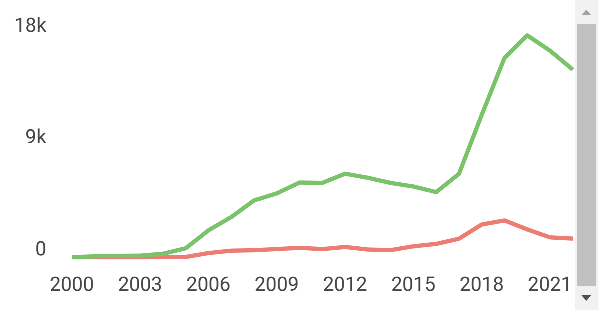

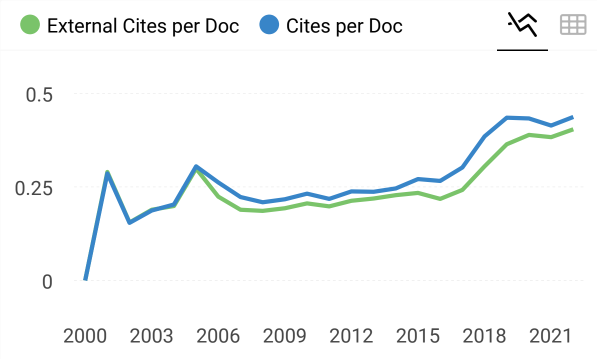

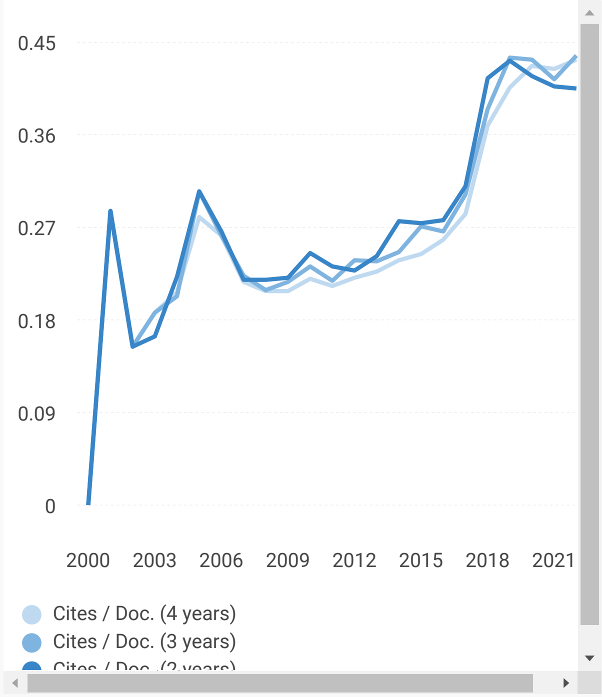

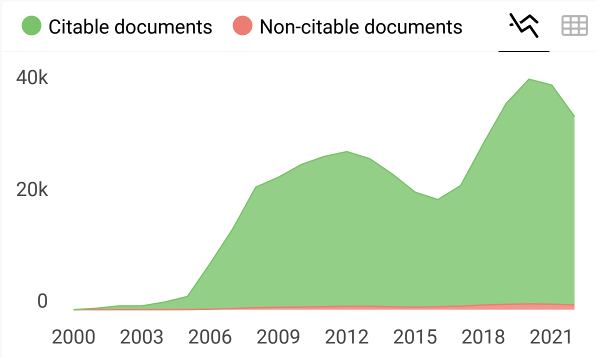

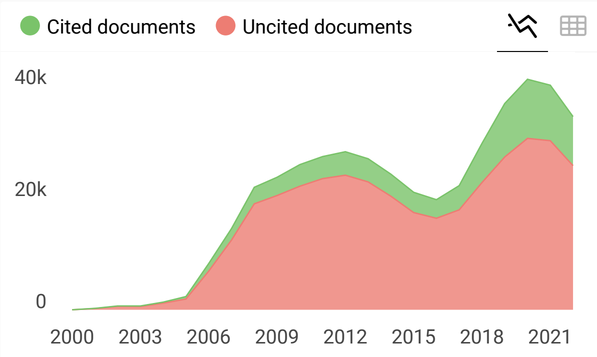

← Show this widget in your own website

Just copy the code below and paste within your html code:

<a href="https://www.scimag

SCImago Graphica

Explore, visually communicate and make sense of data with our **new data visualization tool**.

Metrics based on Scopus® data as of April 2023

A **akhmed** 4 months ago

AIP Conference Proceedings

scitation.org/journal/apc

Volume 2403

THERMOFLUID XI

Proceedings of the 11th International Conference on Thermofluids 2020

Yogyakarta, Indonesia • 10–11 November 2020

Editors • Indarto, Samsul Kamal, Harwin Saptoadi, Sutrisno, Deendarlianto and Khasani

thermofluid XI

11 TH INTERNATIONAL CONFERENCE ON THERMOFLUIDS 2020

AIP Publishing

Organizing Committee

Scientific Committee

Prof. Indarto (Universitas Gadjah Mada, Indonesia)

Prof. Samsul Kamal (Universitas Gadjah Mada, Indonesia)

Prof. Harwin Saptoadi (Universitas Gadjah Mada, Indonesia)

Assoc. Prof. Chong Wen Tong (University of Malaya, Malaysia)

Dr.-Ing. Marco Jose da Silva (Federal University of Technology – Paraná, Brazil)

Assoc. Prof. Leong Kai Choong (Nanyang Technological University, Singapore)

Prof. Agus Pulung Sasmito (McGill University, Canada)

Prof. Tetsuya Suekane (Tokyo Institute of Technology, Japan)

Steering Committee

Prof. Indarto (Professor in Fluid Dynamics & Energy Conversion, UGM)

Prof. Harwin Saptoadi (Professor in Energy Conversion, UGM)

Prof. Samsul Kamal (Professor in Heat and Mass Transfer, UGM)

Prof. Sutrisno (Professor in Fluid Mechanics, UGM)

Prof. Deendarlianto (Director of Center for Energy Studies UGM)

Dr. Tri Agung Rohmat (Head of Energy Conversion Lab., UGM)

Dr. Adhika Widyaparaga (Head of Fluid Mechanics Lab., UGM)

Dr. Joko Waluyo (Head of Heat & Mass Transfer Lab., UGM)

Dr. Jayan Sentanuhady (Head of Innovation Center for Automotive UGM)

Chair

Dr. Khasani, S.T., M.Eng.

Vice-Chair

Willie Prasidha, S.T., M.Eng.

Publication and proceeding

Willie Prasidha, S.T., M.Eng.

THERMOFLUID XI
AIP Conf. Proc. 2403, 010002-1–010002-7; https://doi.org/10.1063/12.0007287
Published by AIP Publishing. 978-0-7354-4167-5/$30.00

Issues

Select Decade 2020

Select Year 2021

Issue 2 December - Volume 2403, Issue 1

PRELIMINARY

AUTOMOTIVE ENGINEERING

COMBUSTION AND AUTOMOTIVE ENGINEERING

Numerical simulations of biogas flames using OpenFOAM

R. Nivethana Kumar; V. Raghavan

AIP Conference Proceedings 2403, 030003 (2021) https://doi.org/10.1063/5.0071011

Abstract View article PDF

FLUID DYNAMICS

CFD simulation for investigating the effect of coal size on tangentially coal fired boiler combustion

Nur Ikhwan; Wawan Aries Nugroho; Vivien Suphandani; Ardi Nugroho

AIP Conference Proceedings 2403, 040001 (2021) https://doi.org/10.1063/5.0070721

Abstract View article PDF

CFD study of damaged blade effect on the gas turbine meter performance

Zulkarnaen; Deendarlianto; Indarto

AIP Conference Proceedings 2403, 040002 (2021) https://doi.org/10.1063/5.0073998

Abstract View article PDF

Characteristics of fluid flow in fixed-bed reactor models composed of spherical and porous tubular milli-sized particles

Ridwan P. Putra; Dhyna Analyes Trirahayu; Khairul Hadi Burhan; Fauzian Ichsan; Mubiar Purwasasmita

AIP Conference Proceedings 2403, 040003 (2021) https://doi.org/10.1063/5.0070681

Abstract View article PDF

Computer aided investigation on the effect of internal surface micro grooving for enhanced thermal management of heat exchanger

Mohamed Moustafa Abdelhalim Ahmed Eid; Mohd Nashrul Mohd Zubir; Mohd Ridha Bin Muhamad; Kazi Md. Salim Newaz

AIP Conference Proceedings 2403, 040004 (2021) https://doi.org/10.1063/5.0070873

Abstract View article PDF

Design and analysis of single-stage axial mini turbine for UAV jet engine

Muhammad Agung Bramantya; Adam Muhammad Fadhillah

AIP Conference Proceedings 2403, 040005 (2021) https://doi.org/10.1063/5.0071110

Abstract View article PDF

Design and CFD simulation of centrifugal compressor for mini jet-turbine engine 200 N thrust

Sint Helent Dinara; Muhamad Agung Bramantya

AIP Conference Proceedings 2403, 040006 (2021) https://doi.org/10.1063/5.0073978

Abstract View article PDF

Determination of absolute roughness under transient condition in gas transmission pipeline 🛒

M. Subhan Missuari; Deendarlianto; Indarto

AIP Conference Proceedings 2403, 040007 (2021) https://doi.org/10.1063/5.0071488

Abstract View article PDF

Effect of camber line variations on open flume turbine performance 🛒

Warjito; Budiarso; Kevin Kameswara; Sanjaya B. S. Nasution; Muhammad Farhan Syahputra

AIP Conference Proceedings 2403, 040008 (2021) https://doi.org/10.1063/5.0071107

Abstract View article PDF

Effect taper ratio on V-tail configuration of unmanned aerial vehicle 🛒

Muhammad Agung Bramantya; Ega Nanda Arda Janitra

AIP Conference Proceedings 2403, 040009 (2021) https://doi.org/10.1063/5.0071109

Abstract View article PDF

Experimental study of *Swirl Microbubble Generator* with 1.2 millimeter diameter of gas nozzle and 1 millimeter distance to the outlet 🛒

Drajat Indah Mawarni; Kyla Alcia Tambunan; Indarto; Deendarlianto

AIP Conference Proceedings 2403, 040010 (2021) https://doi.org/10.1063/5.0071083

Abstract View article PDF

Far field flow simulation of contra-rotating H-Darrieus vertical axis wind turbine 🛒

B. Ko; S. Liu; Z. Fang; B. Nugroho; R. C. Chin

AIP Conference Proceedings 2403, 040011 (2021) https://doi.org/10.1063/5.0070675

Abstract View article PDF

Numerical evaluation of minimum residence time in a delay chamber using scale-down model 🛒

Hanapi Ali; Warjito

AIP Conference Proceedings 2403, 040012 (2021) https://doi.org/10.1063/5.0070687

Abstract View article PDF

Performance comparison of centrifugal pump in variation of impeller blade number through numerical simulation 🛒

Joko Waluyo; Rahmat Waluyo

AIP Conference Proceedings 2403, 040013 (2021) https://doi.org/10.1063/5.0074344

Abstract View article PDF

The effect of measurement results flue gas emission with and without using flow straightener on stack 🛒

Dewi Puspitasari; S. Brilliant; E. Ellyanie; W. Erick; M. Marwani; M. Irsyad H.

AIP Conference Proceedings 2403, 040014 (2021) https://doi.org/10.1063/5.0074064

Abstract View article PDF

HEAT TRANSFER AND PHASE CHANGE

A simulation and experimental study on particle volume fraction of PMMA suspension in centrifugal fields

Yosephus Ardean Kurnianto Prayitno; Tong Zhao; Yoshiyuki Iso; Masahiro Takei

AIP Conference Proceedings 2403, 050001 (2021) https://doi.org/10.1063/5.0070737

Abstract View article PDF

MULTIPHASE FLOW

Time-series differential pressure fluctuations of a flooding regime: A preliminary experimental results investigation on a 1/30 down-scaled PWR hot leg geometry

Achilleus Hermawan Astyanto; Yusuf Rahman; Akbar Yuga Adhikara Medha; Deendarlianto; Indarto

AIP Conference Proceedings 2403, 060001 (2021) https://doi.org/10.1063/5.0070772

Abstract View article PDF

Two phases flow regime assignment based on Wavelet features of pressure signal in the airlift pump-bubble generator

I. G. N. B. Catrawedarma; Deendarlianto; Indarto

AIP Conference Proceedings 2403, 060002 (2021) https://doi.org/10.1063/5.0071108

Abstract View article PDF

RENEWABLE ENERGY AND ENERGY HARVESTING

Computer program application to design a cross-flow water turbine

Ibra Ilham Wijaya; Samsul Kamal

AIP Conference Proceedings 2403, 070001 (2021) https://doi.org/10.1063/5.0073981

Abstract View article PDF

The effect of orifice diameter on the water vortex turbine performance by numerical method

Warjito; Ridho Irwansyah; Budiarso; Mu'adz Syawali; Sanjaya B. S. Nasution

AIP Conference Proceedings 2403, 070002 (2021) https://doi.org/10.1063/5.0071486

Abstract View article PDF

Designing of 500 watt wind turbine blades for manufacturing

Mujammil Asdhiyoga Rahmanta; Almas Aprilana

AIP Conference Proceedings 2403, 070003 (2021) https://doi.org/10.1063/5.0070697

Abstract View article PDF

Feasibility on introducing an alternative solar powered propelling system for multi-day fishing boats in Sri Lanka

Oshada Gamage; Chamal Wimalasooriya; Chrismal Boteju; W. K. Wimalsiri

AIP Conference Proceedings 2403, 070004 (2021) https://doi.org/10.1063/5.0070707

Abstract View article PDF

Investigation of reduction of Banki turbine shaft diameter to increase power

Sirojuddin; M. H. Fajar; R. Sukarno

AIP Conference Proceedings 2403, 070005 (2021) https://doi.org/10.1063/5.0071148

Abstract View article PDF

Performance of single-large simulated sunlight for indoor photovoltaic testing

Bayu Utomo; Himma Firdaus; Qudsiyyatul Lailiyah; Winda Sari Ramadhani; Intan Paramudita

AIP Conference Proceedings 2403, 070006 (2021) https://doi.org/10.1063/5.0070718

Abstract View article PDF

THERMODYNAMICS AND ENERGY CONVERSION

Gas turbine power augmentation, Badak LNG case study

Dedi Permana

AIP Conference Proceedings 2403, 080001 (2021) https://doi.org/10.1063/5.0073900

Abstract View article PDF

Thermal and thermodynamic optimization of a porous double layered microchannel heat sink

Saheed Adewale Adio; Ridwan Olawale Olagoke; Timothy Adefemi Alo; Adedotun Emmanuel Olalere; Adam Olatunji Muritala

AIP Conference Proceedings 2403, 080002 (2021) https://doi.org/10.1063/5.0070674

Abstract View article PDF

Time-series differential pressure fluctuations of a flooding regime: A preliminary experimental results investigation on a 1/30 down-scaled PWR hot leg geometry

Cite as: AIP Conference Proceedings **2403**, 060001 (2021); https://doi.org/10.1063/5.0070772
Published Online: 02 December 2021

Achilleus Hermawan Astyanto, Yusuf Rahman, Akbar Yuga Adhikara Medha, et al.

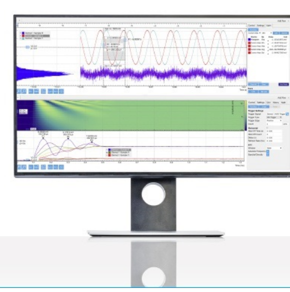

Time-Series Differential Pressure Fluctuations of a Flooding Regime: A Preliminary Experimental Results Investigation on a 1/30 Down-Scaled PWR Hot Leg Geometry

Achilleus Hermawan Astyanto[1, 3, a)], Yusuf Rahman[1)], Akbar Yuga Adhikara Medha[1)], Deendarlianto[1, 2)], and Indarto[1, 2)]

[1] *Department of Mechanical and Industrial Engineering, Universitas Gadjah Mada, Jl. grafika No 2 Kampus UGM, Yogyakarta 55281, Indonesia*
[2] *Center of Energy Studies, Universitas Gadjah Mada, Sekip K-1A Kampus UGM, Yogyakarta 55281, Indonesia*
[3] *Department of Mechanical Engineering, Universitas Sanata Dharma, Kampus III USD, Yogyakarta 55282, Indonesia*

[a)] Corresponding author: achil.herma@mail.ugm.ac.id

Abstract. A nuclear power plant operation requires high safety system designs. Therefore, an accidental scenario such as the SBLOCA should be anticipated well. This particularly also relates to a flow phenomenon occurred during the primary circuit leakage called the counter current flow limitation (CCFL) which probably initiates a flooding regime. This work aims to investigate time-series pressure fluctuations of a flooding regime in a complex geometry representing 1/30 down-scaled of PWR hot leg. Statistical tools i.e. PDF and PSD were assessed to obtain the characteristics of time-series differential pressure fluctuations of the regime. The results obtained imply that the idea proposed are advisable to be assesed more.

Keywords. Time-series differential pressure fluctuations, flooding, PSD, PDF, PWR hot leg.

INTRODUCTION

A pressurized water reactor (PWR) generates nuclear power to produce electricity. It operates at a high pressure and temperature conditions. In its reactor core, called the reactor pressure vessel (RPV), the pressure and temperature reach 15 MPa and 325 °C, respectively. Since these magnitudes are still lower than its critical pressure and temperature, in which for water these will be 22 MPa and 374 °C, the working fluid should be in a liquid phase.

In a PWR, the RPV is connected to a channel called hot leg. It is a channel containing a horizontal pipe, an elbow and an incline section called riser. The RPV and hot leg later form a closed circuit namely primary circuit. The pressurized water at a high temperature flowing through the hot leg is used to heat the water in a steam generator (SG) into a steam. The steam later turns the turbine and produces electricity.

In a reactor accidental scenario, called the small break loss of cooling accident (SBLOCA), even a small leakage on the primary circuit causes suddenly pressure drops. As a result, either partially or totally there will be a phase change in the RPV. The steam which is produced by the phase change later flows along the hot leg through the SG. When the steam reaches the hot leg section which is connected to the SG, as a result of significant temperature difference between the vapor and the fluid temperature in the SG, there will be a heat transfer between the steam and the fluid in the SG. Therefore, the steam will be condensed and produces condensate. Since there is elevation difference, the condensate flows counter currently through the hot leg back to the RPV. Nevertheless, a stratified counter current flow occurs.

THERMOFLUID XI
AIP Conf. Proc. 2403, 060001-1–060001-12; https://doi.org/10.1063/5.0070772
Published by AIP Publishing. 978-0-7354-4167-5/$30.00

Al Issa and Macian (2011) reported that in a stratified counter current flow, the liquid and gas was stable within a certain range. An increasing in gas flow rate gradually disturbed the liquid flow, and later reversed its direction either partially or totally. This phenomenon is called counter current flow limitation (CCFL). Furthermore, Deendarlianto et al. (2011) succeeded to remark that in low gas flow rates, the liquid flowed in an opposite direction along the hot leg. Meanwhile, the pressure differences between the RPV and SG gave low magnitudes, and gradually increased with the increase of the gas flow rates. This flow regime is called a stable counter current flow. When the gas flow rates were gradually increased until the gas mass flow rate in the RPV was equal to the liquid mass flow rate in the inlet, this point was later known as the onset of flooding. The flooding regime is limited by the onset of flooding and zero liquid penetration (ZLP). In the PWR, the flooding and ZLP are two things to be avoided as well. This relates to the safety of the nuclear power plant operations.

Factually, flooding involves complex physical phenomena. The availability of information which supports it to some better understandings are always needed. Nowadays there are still limited theoretical approaches only on this field of study. This indicates that there are so many experimental data would be needed to support it (Deendarlianto et al., 2011). The better understanding in flooding will contribute to studies in design and analytical approaches to the safety of nuclear reactor power plant operation.

Generally in its development, some studies related flooding are performed in such areas of analytical studies and mathematical modelling, computational fluid dynamics (CFD) and also mechanistic modelling based on experimental investigations. Some parameters to be investigated could be the horizontal length to diameter (L/D) ratio (Wongwises, 1996; Navarro, 2005; Badarudin et al., 2018), riser length to diameter (I/D) ratio (Navarro, 2005), the cross sectional area shapes (Shidiqui, 1989; Wongwises, 1994; Petritsch and Mewes, 1999), the channel orientations (Lee and Bankoff, 1983; Ghiaasiaan et al., 1997, Deendarlianto et al., 2005; Navarro, 2005), the entrance and exit geometries, and also the fluid physical properties (Ghiaasiaan et al.,1997; Deendarlianto et al., 2004, 2010; Kinoshita et al., 2011).

Wongwises (1996) performed an experimental study in a complex geometry which contained of horizontal pipe, and elbow and inclined pipe. The diameter of test section was 64 mm with outer and inside curvature radii were 60 mm and 135 mm, respectively. The length of horizontal pipe was 1300 mm. The results showed that the onset of flooding were divided into three regions. The first region showed that the onset of flooding was slower to be reached with the increase on liquid flow rate. In the second region, the onset of flooding was faster to be reached with the decrease on liquid flow rate. Meanwhile in the third region, the onset of flooding tent to be faster with the increase of liquid flow rate.

Navarro (2005) investigated the effect of test section geometries and inlet liquid flow rates on the onset of flooding in various inclination angle of elbow of a PWR hot leg. The same effects were also investigated on partial delivery and zero liquid penetration. Fluid flow rates and fluid temperature, upper tank pressure and pressure different between the upper and lower tanks and water level in three positions along the horizontal part of test section ware also measured. The measurement was held using attenuation of gamma radiation.

Kinoshita et al. (2011) reported the effects of liquid physical properties on CCFL in a scaled-down 1/15 hot leg geometry. Diameter of the test section was 50 mm with 80 mm radius curvature of the elbow. The horizontal and inclined lengths were 430 mm and 60 mm, respectively. A conductance parallel wire technique was carried out to measure the water level along the horizontal part of the test section. Furthermore, Glycerol weight percentages were used to vary the density, viscosity and surface tension of the liquid.

Badarudin et al. (2018) performed experimental studies on interfacial behavior in a down-scaled 1/30 of hot leg PWR. The results showed that the onset of flooding were divided into three regions. The first region showed that the onset of flooding was slower to be reached with the increase on the liquid flow rate. In the second region, the onset of flooding was faster to be reached with the decrease on the liquid flow rate. Meanwhile in the third region, the onset of flooding tent to be faster to be reached with the increase of the liquid flow rate.

According to several earlier investigations, the pressure fluctuations of the upper and lower tank which are represents the RPV and SG of the PWR, respectively, has become one of the parameter that has been largely used to recognize the inception of flooding (Deendarlianto et al., 2005; Al Issa and Macian, 2014; Badarudin et al., 2018). Furthermore, signal processing techniques which enable statistical analysis of the data obtained, is also common in regimes identification (Luo and Lu, 2010; Santoso et al., 2012; Rodrigeues et al., 2020).

METHODOLOGY

The test section of this experiment was a complex geometry representing a 1/30 down-scaled PWR hot leg. It contains a horizontal pipe, en elbow and riser. The horizontal pipe diameter and length were 25.4 mm and 455 mm, respectively. The elbow's inclination angle was 50° to the horizontal. Meanwhile, the riser lenght to inner diameter (I/D) ratio used was 6.2. FIGURE 1 shows the test section geometry.

FIGURE 2 presents the experimental apparatus. Amount of water from a reservoir tank was pumped into a supply tank using a centrifugal type pump from Grundfos with a maximum flow rate of 283 lpm at 2790 rpm. As a result of gravitational force, water flowed through three parallel pipes. The water flow rates were regulated by valves. The magnitudes were read from each water rotameter which was applied on certain distance after each valve. Water then flowed into the upper tank. From the upper tank, the water flowed through hot leg into the lower tank.

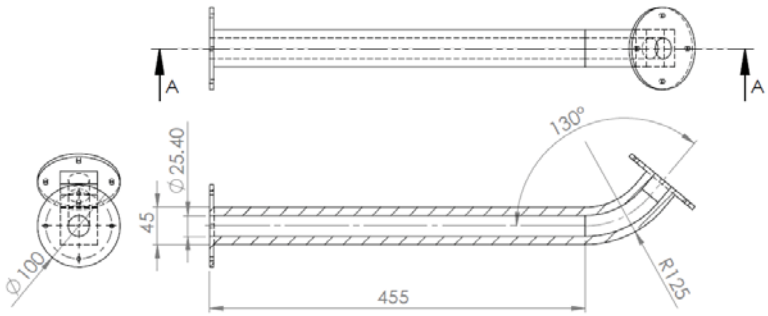

FIGURE 1. The test section geometry.

On the other hand, the air was supplied by torax type air compressor from Shark with a maximum flow rate of 0.1 m^3/s at 530 rpm. A pressure regulator was also installed to maintain the air pressure to a constant pressure system of 50 psi. Two air flowmeters with a total volumetric flow rate of 135 lpm were applied parallel to read the informations related the air flow rates. Later, the air entered the lower tank, flowed along the hot leg into upper tank and then leave the system to the atmospher.

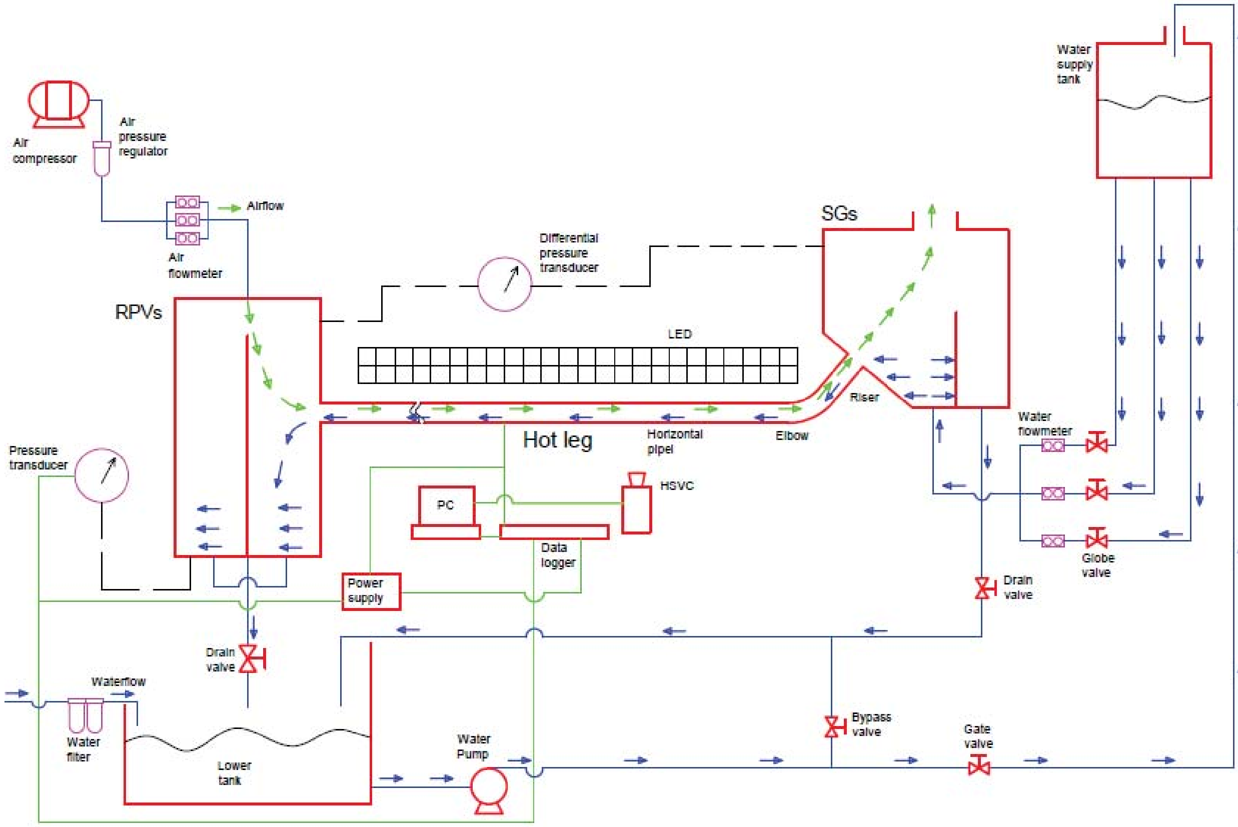

FIGURE 2. The scheme of experimental apparatus.

In the upper and lower tank a set of pressure tap was applied and connected to a differential pressure tranduser (DPT) by Validyne with a measurement range of 80 psi to obtain time series pressure fluctuation signal voltages. The water level in the lower tank was observed using measuring lines, and validated using time series static pressure from another DPT by Validyne with a measurement range of 60 psi. Those DPT were connected to Advantech 4716AE data logger and a personal computer. The liquid flow rates range assessed were 0.1 – 3 lpm. Furthermore, to ensure that the flow was steady after the gas flow rate adjustment, the gas flow rate was kept for 15 seconds before its adjustment to the next increment.

Data tabulated contained the onset of flooding gas and liquid flow rates, while the data acquired included the voltages of the pressure difference fluctuation signals between the RPVs and SGs. Furthermore, the flooding characteristics was expressed in the Wallis parameters (J_K^*). On the other hand, the pressure fluctuation signal analysis were expressed in the both probability density function (PDF) and power spectral density (PSD). Microsoft Excel program features were applied to obtain the time-series pressure difference fluctuations (Pressure, kPa), PDF and PSD graphs with various gas and liquid flow rates.

In order to ensure the advisability of the experimental apparatus, the onset of flooding curve obtained by the present experiment was compared to some earlier data in which the test section had similar geometries i.e. the PWR hot leg from Wongwises (1996), Navarro (2005), Deendarlianto et al. (2008), Kinoshita et al. (2011) and Badarudin et al. (2018). The onset of flooding curve was obtained by applying the dimensionless Wallis parameter of the both gas and liquid superficial velocities.

The Wallis parameter (1969) describes a ratio of inertia to hydrostatic forces (Deendarlianto et al., 2011). This parameter explains that the superficial velocity is the function of the fluid density, gravitational acceleration and channel diameter, and is formulated as:

$$J_K^* = J_K \sqrt{\frac{\rho_K}{gD(\rho_L - \rho_G)}} \quad , \tag{1}$$

$$J_K = \frac{Q_K}{A} \quad . \qquad (2)$$

Here in the Eq. (1) and (2) the subscript K indicates each phase, ρ is the fluid density, g represents the gravitational acceleration, Q is the volumetric flow rate, A represents the cross sectional area, and D is the channel diameter. In this experiment, the fluids used were water as the liquid phase and air as the gas phase. The physical properties of those fluids are shown in TABLE 1.

TABLE 1. The fluids physical properties

Physical properties	**Symbol**	**Water**	**Air**
Fluid density at 30 °C (kg/m^3)	ρ_L, ρ_G	996	1.165
Surface tension (kg/s^2)	σ_L, σ_G	71.97×10^{-3}	-
Dynamic viscosity at 30 °C (kg/m. s)	μ_L, μ_G	7.97×10^{-4}	1.87×10^{-5}

RESULTS AND DISCUSSION

This section presents the main data obtained by the pressure fluctuation signal voltage data acquisitions. An onset of flooding curve is described. It corresponds to the range in which the authors deliver the signal data analyses. Several comparison on the onset of flooding data are also described in a graph which describes the relationship between the dimensionless superficial velocities of each phase. Meanwhile, the pressure fluctuation signal voltages which indicate flooding regime are shown in time-series. From the fluctuations, the amplitudes representing the pressure differential fluctuations were recorded. Furthermore, the signal fluctuations were also processed by describing the PDF and PSD graphs. From the PDF the distributions of the fluctuations were assessed, while from the PSD, the dominant frequencies were obtained.

The Onset of Flooding

The results obtained shows that the onset of flooding can be divided into three regions based on its trend. The first region shows that the increase in water flow rates fasten the onset of flooding. On the other hand, the second region shows that the onset of flooding is rather slower by the increase of water flow rates. This implies that the second region gives benefit during the LOCA scenario. Meanwhile, the third region shows that the onset of flooding tend to faster by the increase of the water flow rates. Furthermore, in agreement with Navarro (2005), there is not a perfect linier curve which is proposed by Wallis (1969). The onset of flooding curve is shown on the FIGURE 3(a).

On its comparison to several earlier research data, it is clearly seen that there is similar trend with several data from Wongwises (1996), Navarro (2005), Deendarlianto et al. (2008), Kinoshita et al. (2011) and also Badarudin et al. (2018) for 0.1 < $(J_L^*)^{1/2}$ < 0.2. Furthermore, for 0.2 < $(J_L^*)^{1/2}$ < 0.28 the trend within this range is still similar in comparison to those trend of the data obtained, except the Wongwises' (1996). Meanwhile, for $(J_L^*)^{1/2}$ > 0.2 it can be seen that there are similar trend, but under predict to the data obtained by Wongwises (1996). FIGURE 3(b) expresses those comparison to several earlier data.

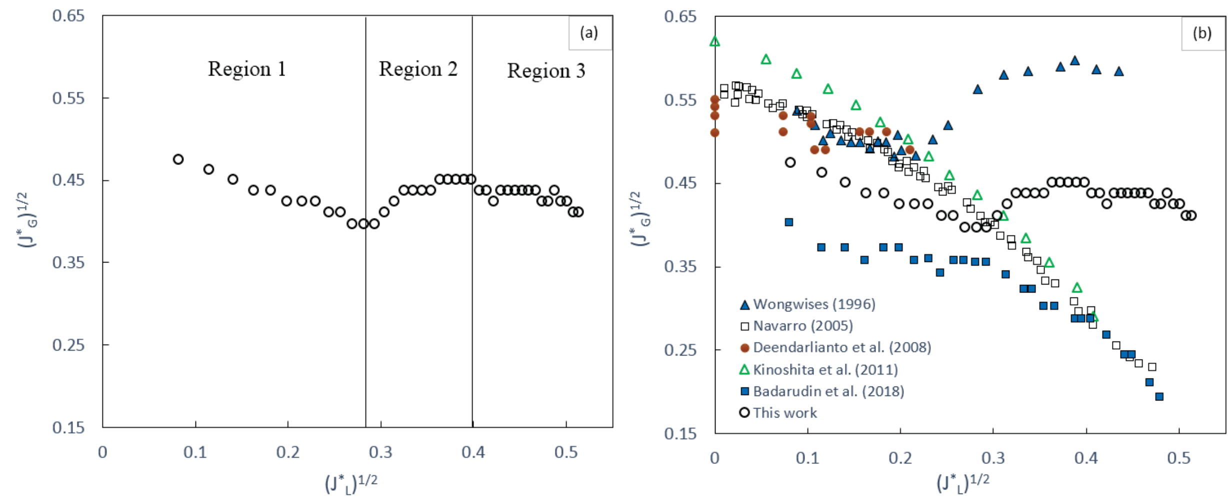

FIGURE 3. (a) The onset of flooding curve (b) Comparison to several earlier studies.

The Time-Series Pressure Fluctuations

Both FIGURE 4 and FIGURE 5 show the time-series pressure fluctuations of several liquid superficial velocities for a given gas superficial velocity and the vice versa, respectively. It can be seen from the graphs that there are not peaks of pressure increasing with the increase of the superficial velocities as reported by Santoso et al. (2012) for a slug flow regime in horizontal co-current flow. Furthermore, an increase of the pressure fluctuation stability with the increase of the J_G as reported by Jaiboon et al. (2013) for a slug flow in the horizontal channel cannot also obtained on the present data. Therefore, based on those flow characteristics, the pressure fluctuations on the present experiment does not indicate the slug flow characteristics as obtained in co-current flow.

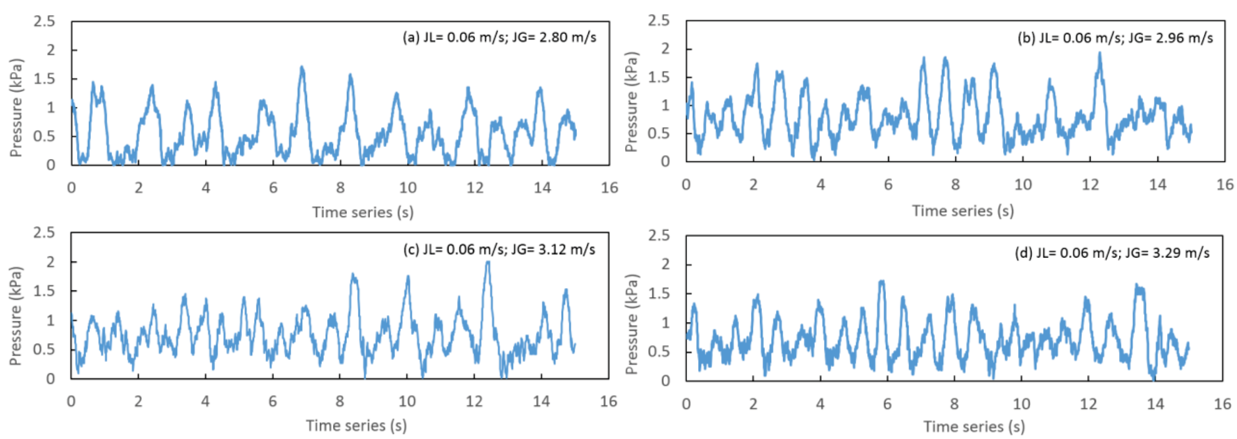

FIGURE 4. The time-series pressure fluctuations of several gas superficial velocities for a given liquid superficial velocity.

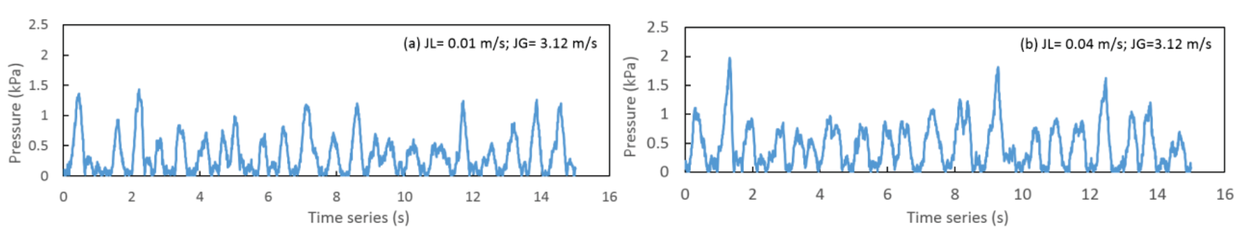

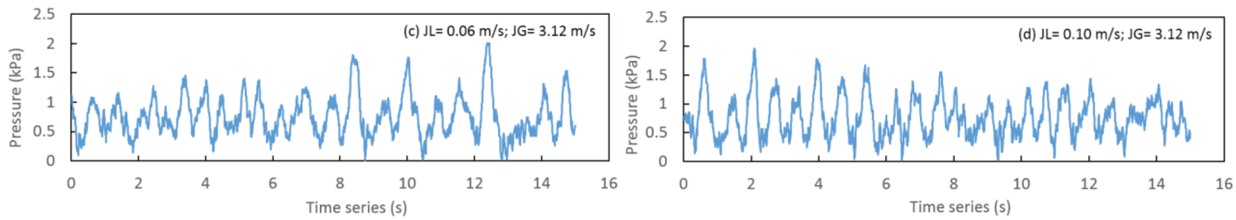

FIGURE 5. The time-series pressure fluctuations of several liquid superficial velocity for a given gas superficial velocity.

The Probability Density Function (PDF)

FIGURE 6 and FIGURE 7 express the PDF graphs of the pressure fluctuations in both for several given liquid and gas superficial velocities, respectively. Those deal with the probability distributions of the time-series pressure fluctuations. It can be obtained from the graphs that the peak of the distributions increase with the increase of gas superficial velocity for the given liquid superficial velocity. These can be observed in several liquid superficial velocities also.

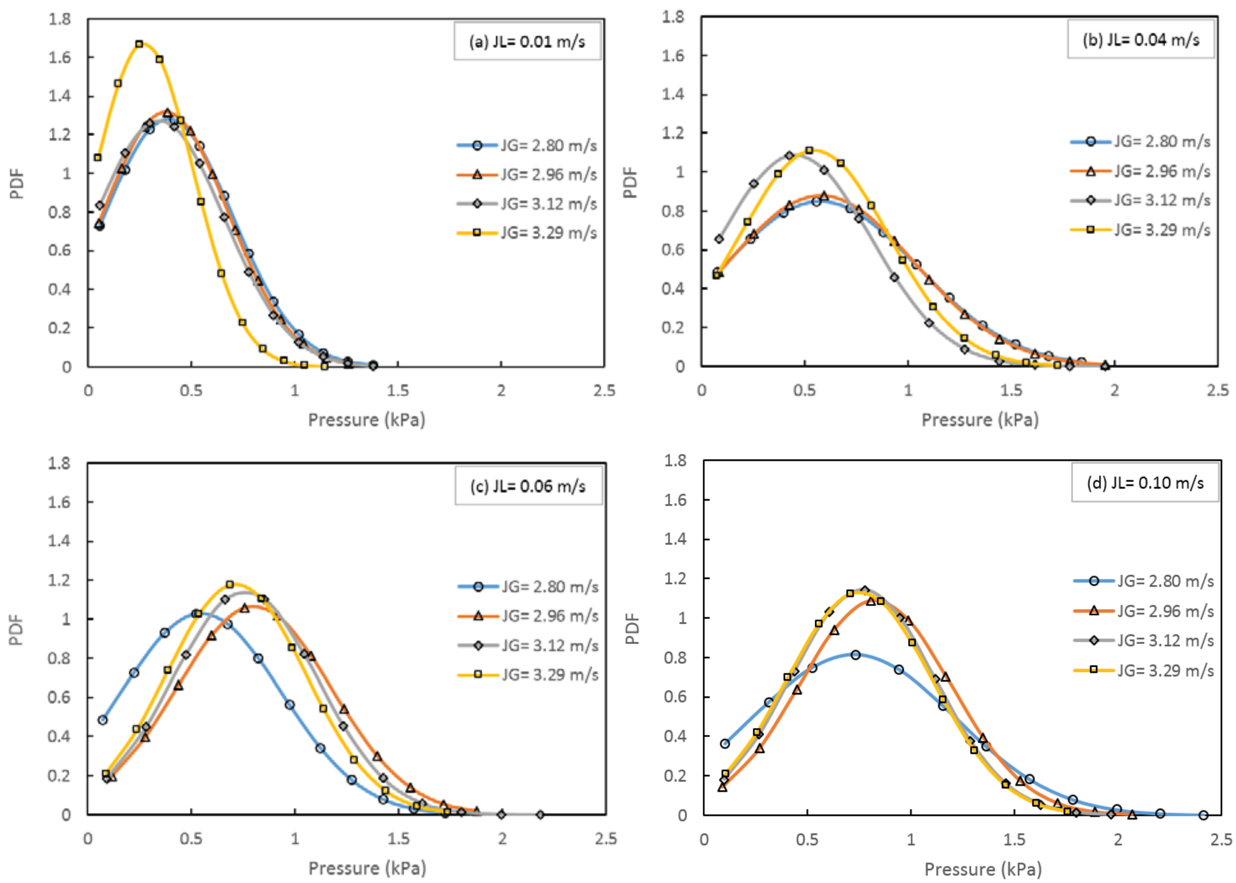

FIGURE 6. The PDF of several gas superficial velocities on several liquid superficial velocities increments.

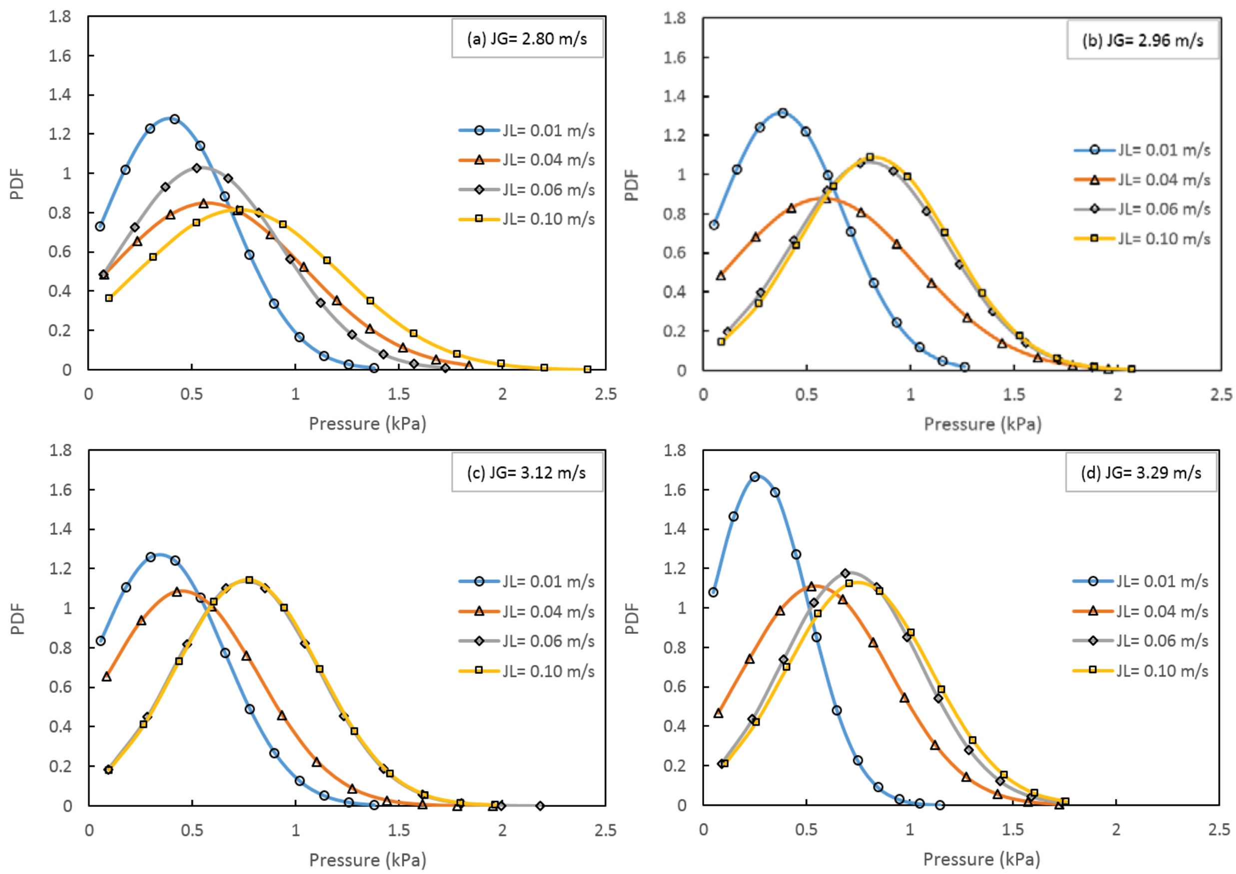

FIGURE 7. The PDF of several liquid superficial velocities on several gas superficial velocities increments.

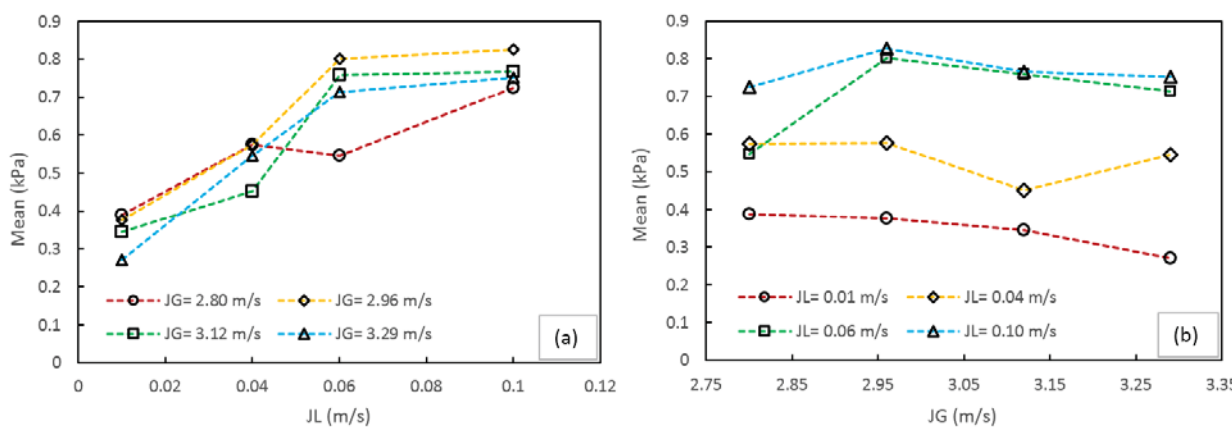

FIGURE 8. The effects of (a) liquid and (b) gas superficial velocities on mean data of pressure fluctuations

FIGURE 8 presents the effects of the both (a) liquid and (b) gas superficial velocities on the mean data of the pressure fluctuations. It can be seen from the FIGURE 8(a) that for almost all gas superficial velocities assessed, the mean data increase with the increase of the liquid superficial velocity. It implies that the pressure difference tends to increase with the increase of the liquid superficial velocity. Only for J_G= 2.80 m/s the mean data decrease with the increase of the liquid superficial velocity from J_L = 0.04 m/s to J_L= 0.06 m/s. Meanwhile, from FIGURE 8(b), it can be seen that only for J_L= 0.01 m/s, the mean data tend to decrease with the increase of the gas superficial velocity.

FIGURE 9 expresses the effects of the both (a) liquid and (b) gas superficial velocities on the standard deviation data of the time-series pressure fluctuations. It can be seen from the FIGURE 9 (b), for J_L= 0.04 and J_L= 0.06 m/s, the standard deviation data decrease with the increase of the gas superficial velocity.

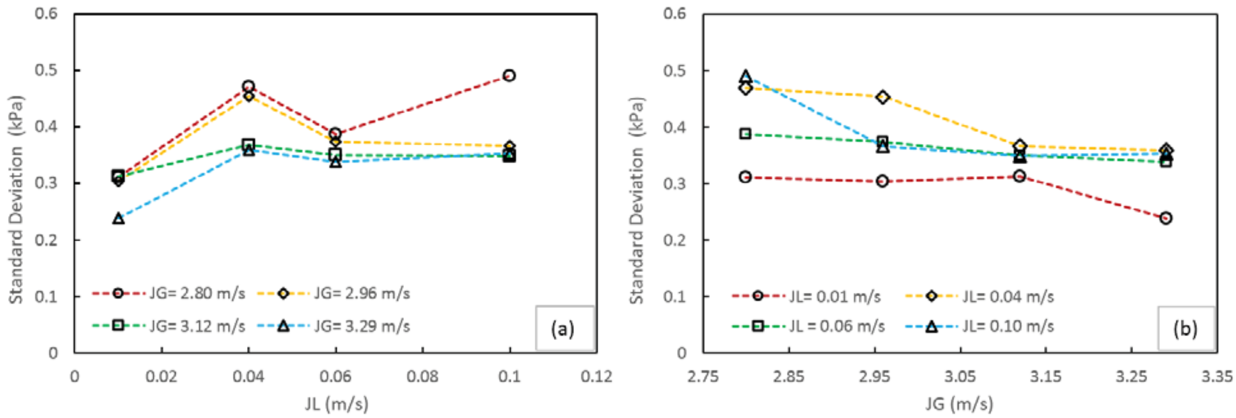

FIGURE 9. The effects of (a) liquid and (b) gas superficial velocities on standard deviation data of pressure fluctuations

The Power Spectral Density (PSD)

FIGURE 10 and FIGURE 11 express the frequencies spectrum obtained by using PSD on time-series pressure fluctuations. In agreement with Arabi et al. (2020), the harmonics frequencies representing the slug frequencies look stochastic. Furthermore, it can also be seen from the FIGURE 10 that the peak of the dominant frequencies move to higher frequencies with the increase of gas superficial velocities in a given liquid superficial velocity. These results are in a contrary with the data obtained by Santoso et al. (2012) which showed the moving of the peak of dominant frequencies to the lower frequencies along the increase of the gas superficial velocities in a given liquid superficial velocity. However, Santoso et al. (2012) conducted their experiment in a co-current terms, meanwhile a flooding regime, despite it contains a co-current flow partially, it basically comes from a countercurrent flow transition.

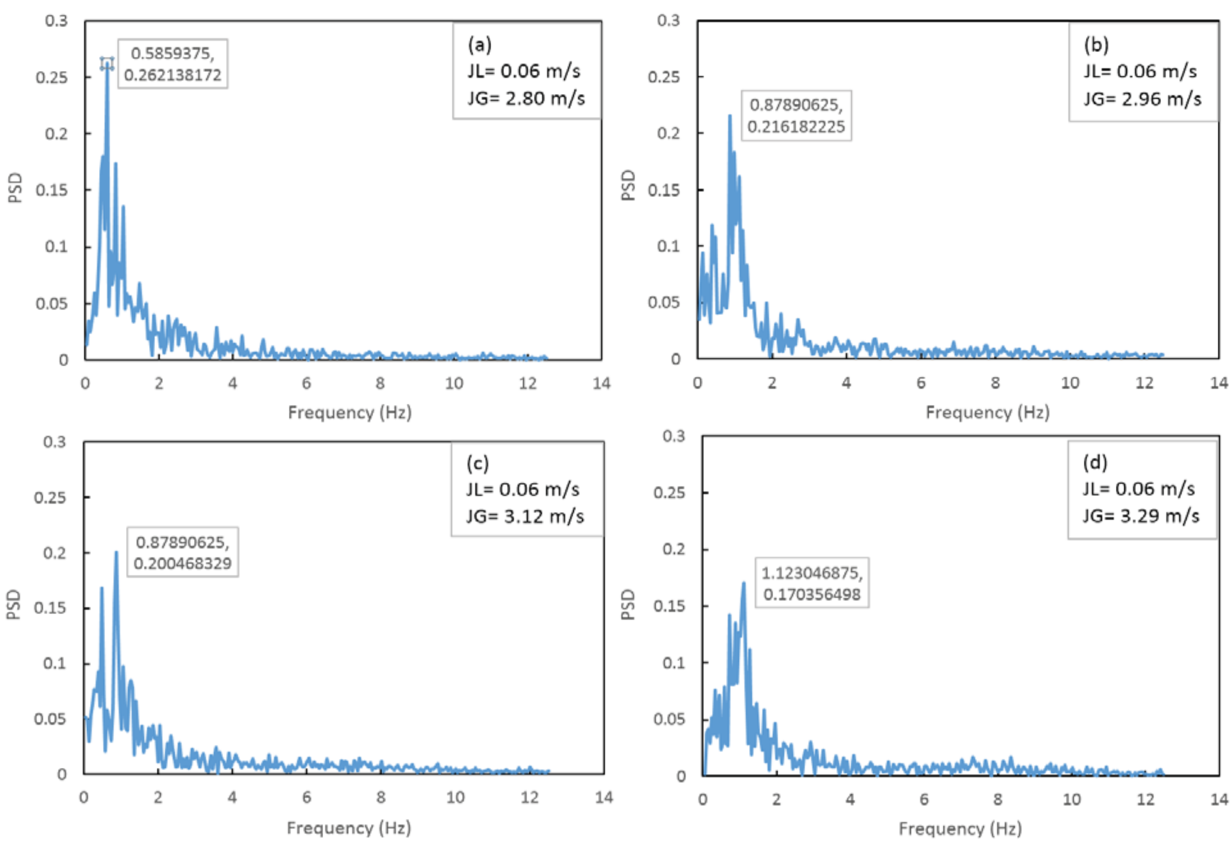

FIGURE 10. The PSD on a given liquid superficial velocity

On the other hand, FIGURE 11 shows PSD graphs of the data frequencies in a given gas superficial velocity. It can be seen that the peak of the dominant frequencies move to the lower frequencies with the increase of liquid superficial velocities. This results are in an agreement with data obtained by Santoso et al. (2012) which showed the moving of the peak of dominant frequency to the lower frequency along the increase of the gas superficial velocity in a given liquid superficial velocity.

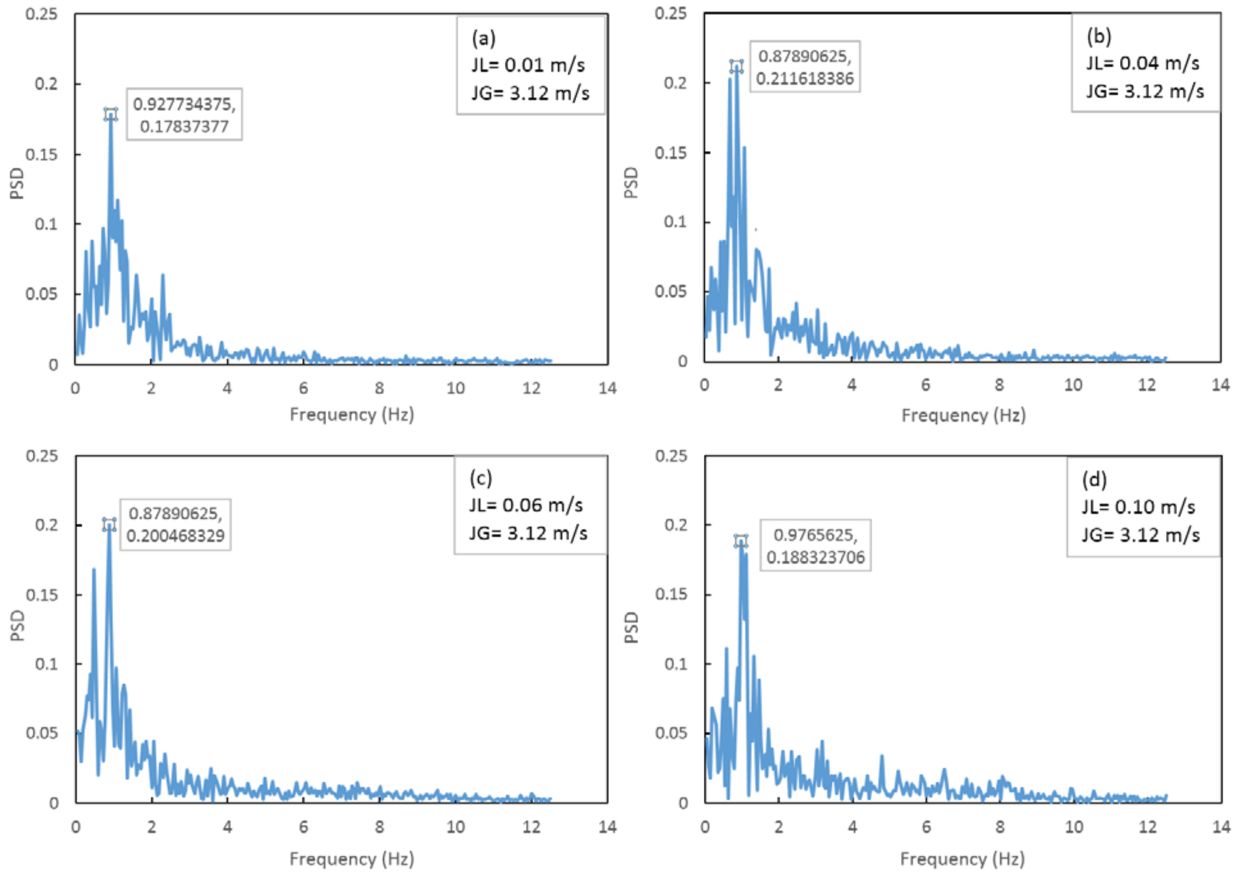

FIGURE 11. The PSD on a given gas superficial velocity

FIGURE 12 presents the effects of both (a) liquid and (b) gas superficial velocities on the dominant frequencies of the time-series pressure fluctuations. Meanwhile, FIGURE 13 presents the effects of both superficial (a) liquid and (b) gas velocities on the maximum PSD of the time-series pressure fluctuations.

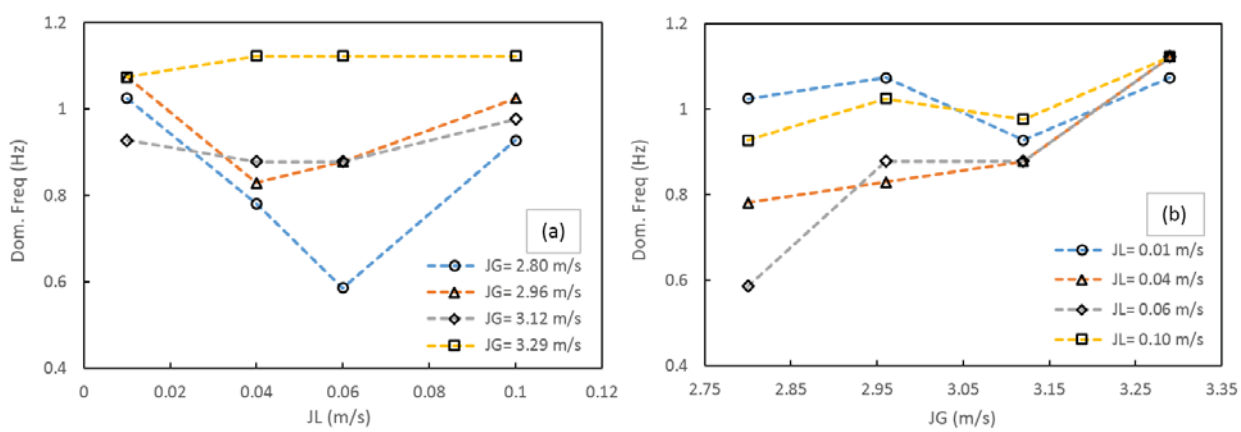

FIGURE 12. The effects of (a) liquid and (b) gas superficial velocities on dominant frequency of pressure fluctuations

It can be seen from the FIGURE 12(b) that for J_L= 0.04 m/s and J_L= 0.06 m/s the dominant frequency and the maximum spectra increase with the increase of the gas superficial velocity. Meanwhile FIGURE 13(a) expresses that only for J_G= 2.8 m/s, the maximum PSD increase with the increase of the liquid superficial velocity. On the other hand, FIGURE 13(b) expresses that only for J_G= 0.06 m/s, the maximum PSD decrease with the increase of the gas superficial velocity.

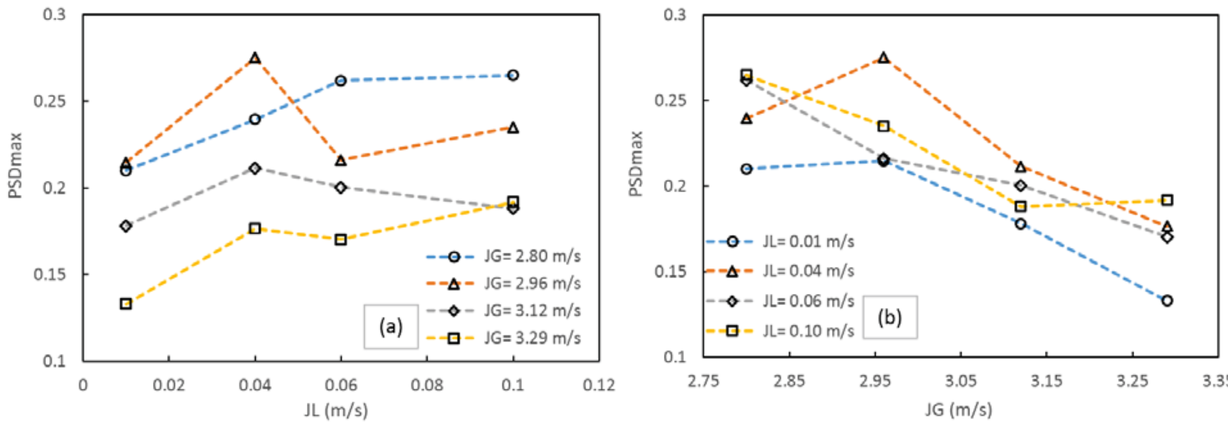

FIGURE 13. The effects of (a) liquid and (b) gas superficial velocities on maximum PSD of pressure fluctuations

CONCLUDING REMARKS

The time-series pressure fluctuations of flooding regimes in a PWR hot leg geometry has been investigated. The data obtained are expressed in terms of both, the onset of flooding curves and several statistical graphs of the pressure fluctuations. The result implies that the second region gives more benefits during the LOCA scenario rather than the first and third regions. The onset of flooding data obtained are also compared to several earlier data from other authors. The comparison shows some agreements with some earlier results. This indicates that the experimental apparatus and the research methodology are advisable to be assesed.

ACKNOWLEDGEMENTS

The authors would like to acknowledge the Direktorat Jenderal Pendidikan Tinggi Kementerian Pendidikan dan Kebudayaan of Republic Indonesia for the scheme of Beasiswa Pascasarjana Dalam Negeri (BPPDN) 2019. This manuscript was written in terms of doctoral academic research series in the Laboratory of Fluid Mechanics, Department of Mechanical and Industrial Engineering, Universitas Gadjah Mada. We also grateful Mr. I Gusti Ngurah Bagus Catrawedarma for several technical supports.

REFERENCES

1. A. Arabi, Y. Salhi, Y. Zenati, E.K. Si-Ahmed, J. Legrand, On gas-liquid intermittent flow in a horizontal pipe: Influence of sub-regime on slug frequency, *Chemical Engineering Science*, Vol. 211: 115251 (2020).
2. A. Badarudin, A. Setyawan, O. Dinaryanto, A. Widyatama, Indarto, Deendarlianto, Interfacial behavior of the air-water counter-current two-phase flow in a 1/30 scale-down of pressurized water reactor (PWR) hot leg, *Annals of Nuclear Energy*, Vol. 116: 376–387 (2018).
3. B. Santoso, Indarto, Deendarlianto, S.W. Thomas, Fluktuasi beda tekanan dari pola aliran slug air-udara pada aliran dua fase searah pipa horizontal, *Jurnal Teknik Mesin Rotasi*, Vol. 14, No. 2: 1–6 (2012).
4. Deendarlianto, C. Vallée, D. Lucas, M. Beyer, H. Pietruske, H. Carl, Experimental study on the air/water counter-current flow limitation in a model of the hot leg of a pressurized water reactor, *Nuclear Engineering and Design*, Vol. 238: 3389–3402 (2008).
5. Deendarlianto, A. Ousaka, Indarto, A. Kariyasaki, D. Lucas, K. Vierow, C. Vallee, K. Hogan, The effects of surface tension on flooding in counter-current two-phase flow in an inclined tube, *Nuclear Engineering and Design*, Vol. 234, 214–233 (2010).

6. Deendarlianto, A. Ousaka, A. Kariyasaki, T. Fukano, Investigation of liquid film behavior at the onset of flooding during adiabatic counter-current air–water two-phase flow in an inclined pipe, *Nuclear Engineering and Design*, Vol. 235: 2281–2294 (2005).
7. Deendarlianto, T. Hohne, D. Lucas, K. Vierow, Gas-liquid countercurrent two-phase flow in a PWR *hot leg*: A comprehensive research review, *Nuclear Engineering and Design*, Vol. 243: 214–233 (2011).
8. G.B. Wallis, "*One-dimensional two-phase flow*", Chapter 11, pp. 336-345, New York, USA, McGraw Hill, (1969)
9. G. Petritsch, D. Mewes, Experimental investigations of the flow patterns in the hot leg of a pressurized water reactor, *Nuclear Engineering and Design*, Vol. 188, 75–84 (1999).
10. H. Siddiqui, S. Banerjee, K.H. Ardron, Flooding in an elbow between a vertical and a horizontal or neat-horizontal pipe, *International Journal of Multiphase Flow*, Vol. 12, No. 4 pp 531–541 (1986).
11. I. Kinoshita, T. Nriai, A. Tomiyama, D. Lucas, M. Murase, Effects of liquid properties on CCFL in a scaled-down model of a PWR hot leg, *Journal of Power and Energy Systems*, Vol. 5, No. 3: 316–329 (2011).
12. M.A. Navarro, Study of countercurrent flow limitation in a horizontal pipe connected to an inclined one, *Nuclear Engineering and Design*, Vol. 235: 1139–1148 (2005).
13. O. Jaiboon, B. Chalermsinsuwan, L. Mekasut, P. Piumsomboon, Effect of flow pattern on power spectral density of pressure fluctuation in various fluidization regimes, *Powder Technology*, Vol. 233, 215–226 (2013).
14. R.L.P. Rodrigues, C. Cozin., B.P. Naidek, M.A.M. Neto, M.J. da Silva, R.E.M. Morales, Statistical features of the flow evolution in horizontal liquid-gas slug flow, *Experimental Thermal and Fluid Science*, Vol. 119:110203 (2020).
15. S. Al Issa, R. Macian, A review of CCFL phenomenon, *Annals of Nuclear Energy*, Vol. 38: 1795–1819 (2011).
16. S. Al Issa, R. Macian, Experimental investigation of countercurrent flow limitation (CCFL)in a large-diameter hot-leg geometry: A detailed description of CCFLmechanisms, flow patterns and high-quality HSC imaging of theinterfacial structure in a 1/3.9 scale of PWR geometry, *Nuclear Engineering and Design*, Vol. 280: 550–563 (2014).
17. S.C. Lee, S.G. Bankoff, Stability of Steam-Water Countercurrent Flow in an Inclined Channel: Flooding, *Journal of Heat Transfer*, Vol. 105/713 (1983).
18. S.M. Ghiaasiaan, X. Wu, D.L. Sadowski, S.I. Abdel-Khalik, Hydrodynamic characteristics of counter-current two-phase flow in vertical and inclined channels: effects of liquid properties, *International Journal of Multiphase Flow*, Vol. 23, No. 6, pp. 1063-1083 (1997).
19. S. Wongwises, Two-phase countercurrent flow in a model of a pressurized water reactor hot leg, *Nuclear Engineering and Design*, Vol. 166: 121–133 (1996).
20. X.M. Luo, Y.L. Lu, "Fluctuation characteristics of gas liquid two phase slug flow in horizontal", *AIP Publishing*, 2010.

thermofluid XI
11 TH INTERNATIONAL CONFERENCE ON THERMOFLUIDS 2020

Departemen Teknik Mesin dan Industri

CERTIFICATE

This certificate is hereby awarded to

Achilleus Hermawan Astyanto, Yusuf Rahman, Akbar Yuga Adhikara Medha, Deendarlianto, and Indarto

for his/her paper

Time-series differential pressure fluctuations of a flooding regime: A preliminary experimental results investigation on a 1/30 down-scaled PWR hot leg geometry

at Thermofluid XI: 11th International Conference on Thermofluid 2020
conducted on 10th-11th November 2020

Prof. Ir. M. Noer Ilman, S.T., M.Sc., Ph.D., IPM
(Head of Department Mechanical and Industrial Engineering UGM)

Dr. Ir. Khasani, S.T., M.Eng., IPM
(Chief Coordinator of Thermofluid XI)

thermofluid XI
11 TH INTERNATIONAL CONFERENCE ON THERMOFLUIDS 2020

Departemen Teknik Mesin dan Industri

CERTIFICATE

This certificate is hereby awarded to

Achilleus Hermawan Astyanto

As Paper Presenter

Time-series differential pressure fluctuations of a flooding regime: A preliminary experimental results investigation on a 1/30 down-scaled PWR hot leg geometry

at Thermofluid XI: 11th International Conference on Thermofluid 2020 conducted on 10th-11th November 2020

Prof. Ir. M. Noer Ilman, S.T., M.Sc., Ph.D., IPM
(Head of Department Mechanical and Industrial Engineering UGM)

Dr. Ir. Khasani, S.T., M.Eng., IPM
(Chief Coordinator of Thermofluid XI)